

## Domains and Distances in Magnetic Systems

Avidan U. Neumann

*Laboratoire de Physique Statistique de l'E.N.S., 24 rue Lhomond,  
F-75231 Paris Cedex 5, France*

and

*Department of Physics, Bar Ilan University, 52100 Ramat Gan, Israel*

Bernard Derrida

*Laboratoire de Physique Statistique de l'E.N.S., 24 rue Lhomond,  
F-75231 Paris Cedex 5, France*

and

*Service de Physique Théorique de Saclay,  
F-91191 Gif-sur-Yvette Cedex, France*

Gérard Weisbuch

*Laboratoire de Physique Statistique de l'E.N.S., 24 rue Lhomond,  
F-75231 Paris Cedex 5, France*

**Abstract.** When one compares the time evolution of two spin configurations subjected to the same thermal noise, domains appear of identical and opposite spins. We study these domains and their growth for three magnetic systems in two dimensions: ferromagnet, spin glass, and non-symmetric spin glass. For ferromagnets, these distance associated domains are very similar to the magnetic domains. For spin glasses, they have a larger structure than the clusters of frozen spins and they move in time. For non-symmetric spin glasses, small distance associated domains move quickly whereas there are no frozen spins.

### 1. Introduction: the distance method

Dynamical phase transitions have recently been observed in a large variety of magnetic systems when studying the time evolution of distances between two spin configurations subjected to the same thermal noise [1]. The systems which have been investigated so far by this technique include: ferromagnets [1–3], spin glasses in two and three dimensions [1,3], and incommensurate systems [4] (the ANNNI model). In its zero temperature version, the same method has also been used to study networks of boolean automata [5–10] and neural nets [11–13].

In the case of dynamical phase transitions occurring at a finite temperature  $T_c$ , two regimes are observed for the distance in the long time limit. In both regimes, the spin configuration  $\{S_i(t)\}$  at time  $t$  depends both on the initial configuration and on the applied noise between times 0 and  $t$ . At high temperature, the effect of noise is strong enough to make the system forget its initial condition. Therefore, two different configurations subjected to the same thermal noise quickly become identical and their distance vanishes. At low temperature, the distance between the two configurations remains finite. Several effects can be responsible for this non-zero distance: either the configurations belong to two valleys in phase space separated by high energy barriers, like in the case of ferromagnets; or, because of a chaotic dynamics with a tendency for close trajectories in phase space to diverge, the configurations end up at a finite distance, like in networks of automata [5–10], or non-symmetric spin glasses [11–14].

Several approaches have been used to locate the transition temperature: for infinite range models (mean field models) [2], or for randomly diluted models [5,11–14], it is possible to write exact equations which give the time evolution of the distance.  $T_c$  is then analytically determined. For finite dimensional systems, only Monte-Carlo simulations have been used so far to compute the distance [1,3,4,6–8,15]. With the help of finite size scaling it is possible to determine  $T_c$  and the critical exponents rather accurately [3].

Only global properties have been studied so far, except in the case of boolean automata on a lattice [6]. Questions arise about the possible existence of spatial structures: are the spins which differ between the two configurations uniformly distributed in space or clustered? Are those spins frozen, or do they flip often in time? What is the time evolution of the spatial structures? Are they moving? What is the relation between these distance related spatial structures and magnetic domains?

The aim of this article is to show these spatial structures, obtained by computer simulations of ferromagnets and symmetric and non-symmetric spin-glasses. Since the programming techniques are different from those aimed at getting good statistics, this work is limited to the exhibition of spatial structures without any attempt to measure quantities averaged on a large number of samples.

The paper is organized as follows: section 2 describes the algorithm used for the dynamics and introduces the various quantities that are displayed in the following sections. Section 3 is devoted to 2 dimensional ferromagnets. Section 4 and 5 are devoted to the 2 dimensional symmetric and non-symmetric spin glasses.

## 2. Heat bath dynamics

Let us briefly recall in this section the parallel heat bath algorithm to be used in this work. All our calculations are done for Ising spins ( $S_i = \pm 1$ ), on a square lattice of linear size  $L = 100$ , with periodic boundary conditions in both directions. Each spin interacts with its four nearest neighbors on the

lattice. The coupling constants  $J_{ij}$  between neighboring spins are  $+1$  in the case of ferromagnets, and  $+1$  or  $-1$  at random for spin glasses. Symmetric spin glasses have equal  $J_{ij}$  and  $J_{ji}$ , while non-symmetric spin glasses have independent  $J_{ij}$  and  $J_{ji}$ .

In this paper we use parallel dynamics based on the heat bath method. To obtain  $\{S_i(t+1)\}$  at time  $t+1$  from  $\{S_i(t)\}$  at time  $t$ , one computes all the updating probabilities  $p_i(t)$  by

$$p_i(t) = \frac{1}{2} + \frac{1}{2} \tanh \left[ \frac{1}{T} \sum_j J_{ij} S_j(t) \right] \quad (2.1)$$

where  $T$  is the temperature, and one updates all the spins by

$$\begin{aligned} S_i(t+1) &= +1 && \text{with probability } p_i(t) \\ S_i(t+1) &= -1 && \text{with probability } 1 - p_i(t) \end{aligned} \quad (2.2)$$

In practice, at each time step  $t$ , we choose for each site  $i$  a random number  $z_i(t)$  uniformly distributed between 0 and 1 and we calculate  $S_i(t+1)$  by

$$S_i(t+1) = \text{sign} \left[ \frac{1}{2} + \frac{1}{2} \tanh \left( \frac{1}{T} \sum_j J_{ij} S_j(t) \right) - z_i(t) \right] \quad (2.3)$$

When we say that we compare the evolution of two different configurations  $\{S_i(t)\}$  and  $\{S'_i(t)\}$  subjected to the same thermal noise, we mean that we use exactly the same set of random numbers  $z_i(t)$  and the same interactions  $J_{ij}$  to update the two configurations and therefore

$$S'_i(t+1) = \text{sign} \left[ \frac{1}{2} + \frac{1}{2} \tanh \left( \frac{1}{T} \sum_j J_{ij} S'_j(t) \right) - z_i(t) \right] \quad (2.4)$$

In this paper we usually start our calculations with uncorrelated random configurations  $\{S_i(0)\}$  and  $\{S'_i(0)\}$  (figures 2–6). Starting with random opposite configuration ( $\{S_i(0)\} = \{-S'_i(0)\}$ ), the same behavior is observed. For figure 7 we start with two configurations which are identical outside an horizontal strip, and opposite inside.

Parallel dynamics are more convenient than sequential dynamics for computer simulations (in particular because it allows one to vectorize the programs). Most of the physical properties are identical to those obtained by sequential dynamics: same critical temperature at equilibrium, same magnetization [3]. There are however a few properties which are different between these two kinds of dynamics [1,3], in particular, for parallel dynamics, the two sublattices of the square lattice are not correlated at a given time. They can be considered as independent events; there are only correlations between a sublattice at time  $t$  and the other sublattice at time  $t+1$ , because all the

information contained in one sublattice at time  $t$  is transferred at time  $t + 1$  to the other sublattice. Therefore, in order to avoid to show pictures of two uncorrelated sublattices, all the pictures presented in this paper show one sublattice at time  $t$  and the other sublattice at time  $t - 1$ .

Let us now describe the quantities which are represented in the next sections. The first quantities that one can consider are, of course, the instantaneous magnetizations  $\{S_i(t)\}$  and  $\{S'_i(t)\}$  at time  $t$  (they are represented in figure 2, columns b and c). From these, it is easy to get the instantaneous distance  $d_i(t)$  between the two configurations

$$\begin{aligned} d_i(t) &= 1 && \text{if } S_i(t) = -S'_i(t) \\ d_i(t) &= 0 && \text{if } S_i(t) = S'_i(t) \end{aligned} \quad (2.5)$$

represented in figure 2 column a, figures 4, 5, 6 column b, and figure 7 columns a, b, c. In order to get some information on the time evolution of spatial structures, we will also show averages over time of the magnetization:

$$\begin{aligned} m_i(t) &= \frac{1}{t} \sum_{t'=1}^t S_i(t') \\ m'_i(t) &= \frac{1}{t} \sum_{t'=1}^t S'_i(t') \end{aligned} \quad (2.6)$$

represented in figure 3, columns b, c. The distance averaged over time

$$c_i(t) = \frac{1}{t} \sum_{t'=1}^t d_i(t') \quad (2.7)$$

is represented in figures 3, 4, 5, 6 column a.

Lastly, since in spin glass systems one does not expect much structure for the magnetization, we decided to show a quantity  $f_i(t)$ , to be further called the flipping rate, defined by the absolute value of the average magnetization  $m_i(t)$ :

$$f_i(t) = |m_i(t)| \quad (2.8)$$

represented in figure 4,5,6, column c.

If  $f_i(t)$  is close to 1, this means that the spin  $S_i(t)$  is almost frozen, whereas if  $f_i(t)$  is close to zero, this means that this spin is much more flipping. In preliminary tests we also measured how many times each spin flips and we observed structures very similar to those obtained with  $f_i(t)$ . Simulations were done on a SUN 3/110 computer and took about 2 hours for 6250 steps for two configurations of  $100 \times 100$  spins. The grey scale for all quantities  $S_i$ ,  $d_i$ ,  $m_i$ ,  $c_i$ , and  $f_i$  is defined on figure 1.

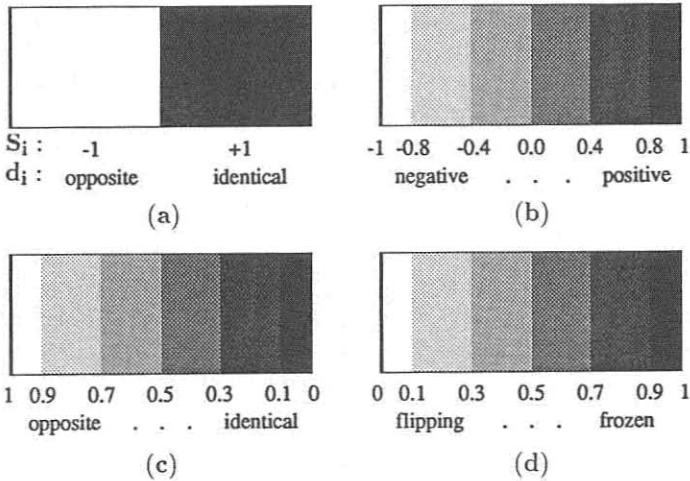


Figure 1: Grey levels used to code the various quantities displayed on the following figures. (a) Instantaneous quantities,  $S_i, d_i$ . (b) Averaged magnetization,  $m_i$ . (c) Averaged distance,  $c_i$ . (d) Flipping rate,  $f_i$ .

### 3. Ferromagnets

Since our simulations are done by quenching random configurations at a temperature below the critical point ( $T_c \approx 2.27$ ), one expects to observe magnetic domains which grow with time (for a review see reference [15]). Figure 2 refers to a  $100 \times 100$  lattice at a temperature of 1.5. It displays the time evolution of the instantaneous magnetizations,  $\{S_i(t)\}$  and  $\{S'_i(t)\}$ , of two random initial configurations, on the right columns (b and c) of frames, and of their distance  $d_i(t)$ , on the left column (a). Time increases from the upper row to the bottom row. For this figure 2, as for figures 3, 4, 6 and 7, time is 10 for the first row, 50 for the second, 250 for the third, 1250 for the fourth and 6250 for the bottom row. On magnetization frames, black corresponds to +1 spins, and white to -1 spins. On distance frames, black corresponds to parallel spins ( $S_i(t) = S'_i(t)$ ) and white to opposite spins ( $S_i(t) = -S'_i(t)$ ).

As expected, we observe on the right columns the growth of magnetic domains, ending with a single domain at the latest times. Apart from their growth, the domains do not seem to move in space with time. One can check that when the configurations are identical, the same fluctuations appear on both domains. We can see that for the ferromagnet, the domain structure associated to the distance (column a) looks similar in shape to the magnetic domains (columns b and c). This shows that the distance  $d_i(t)$  is a quantity

of the same nature as the magnetization [2,3,16].

Figure 3 is obtained with different initial conditions and represents the time evolution of quantities averaged in time from the beginning of the simulation: the two right columns (b and c) represent the averaged magnetizations,  $m_i(t)$  and  $m'_i(t)$ , of the two configurations and the left one (a) their average distance  $c_i(t)$ . In both cases, two domains are still present at time  $t = 6250$ . The effect of averaging over time is to smooth the frontiers of the domains. The fact that very little grey is present on the picture is an indication that the domains do not drift.

Simulations at higher temperatures show that above  $T_c \approx 2.27$ , the average magnetization frames become grey in the long time limit, which means that the average magnetization is 0, and the distance frames become black, indicating that the two configurations merge.

#### 4. Symmetric spin glasses

Figure 4 displays from left to right, the time evolution of the time-averaged distance between two configurations  $c_i(t)$ , the instantaneous distance  $d_i(t)$ , and the flipping rate  $f_i(t)$  of a  $100 \times 100$  symmetric spin glass lattice. Temperature is 0.9, which is below  $T_c \approx 1.7$  [3], the dynamical transition temperature for spin glasses. Colour coding for distance frames is the same as for the preceding figures. On the flipping frames, white corresponds to flipping spins and black to fixed spins. We see the appearance of spatial structures which develop in time on the distance frames. Small domains appear, which grow in time. Their size is definitely smaller than ferromagnetic domains, and their frontiers look more fractal, even when the distance is averaged over the time. The size of the grey regions indicates that these domains drift in time. Smaller structures also appear on the frames describing the flipping rates, but they do not seem to be simply correlated to the distance related spatial structures: this implies that those parts of the configurations which are identical include both fixed and oscillating spins.

Figure 5 represents, from left to right: the time-averaged distance, the instantaneous distance, and the flipping rate, for increasing temperatures from the top row to the bottom: the rows correspond to  $T = 0.3, 0.6, 0.9, 1.2,$  and  $1.5$ , all at the same time 6250. When temperature is increased the effect of thermal noise becomes stronger. A larger fraction of spins are flipping and the distance between configurations decreases. The spatial structures associated with the distance are bigger and move faster (the last frame of column a is grey because of their motion). Above  $T_c \approx 1.7$ , nonrepresented figures show that the two configurations merge and all the spins are flipping.

#### 5. Non-symmetric spin glasses

Figure 6 displays the time evolution of the time-averaged distance, of the instantaneous distance between two configurations and of the flipping rate of a  $100 \times 100$  non-symmetric spin glass lattice. Temperature is 0.9, below

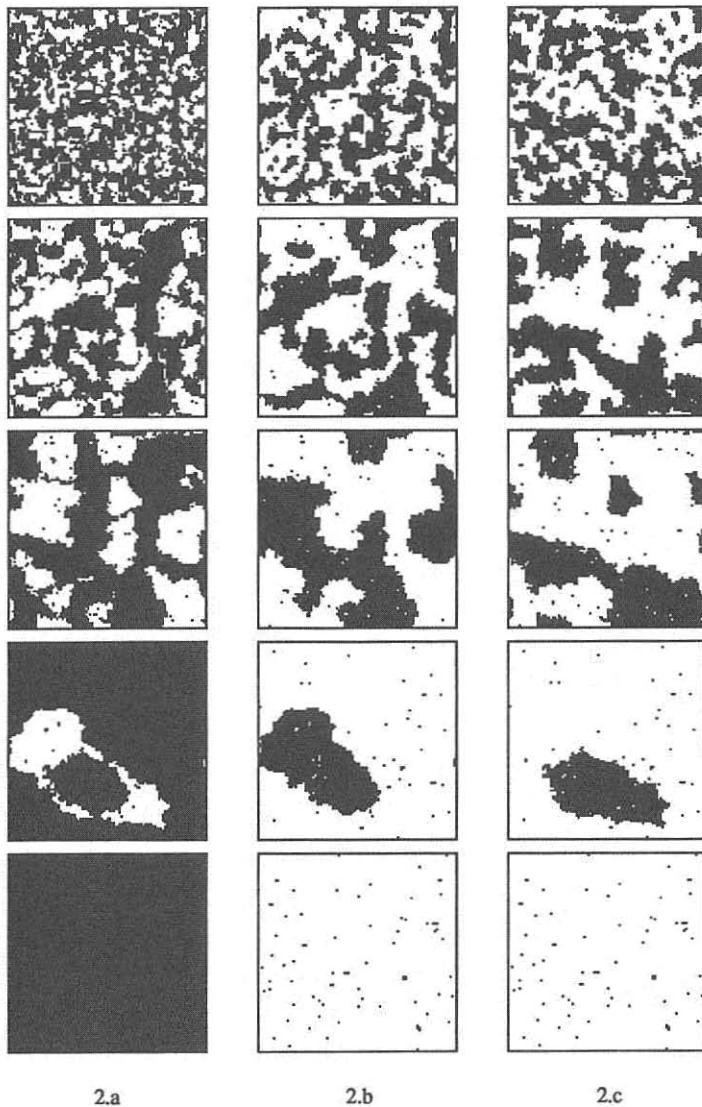


Figure 2: Time evolution of two initially random configurations for the ferromagnet at a temperature of 1.5. Times are from top to bottom 10, 50, 250, 1250, and 6250. (a) Instantaneous distance  $d_i(t)$  between the two configurations. (b) Instantaneous magnetization of the first configuration  $S_i(t)$ . (c) Instantaneous magnetization of the second configuration  $S'_i(t)$ .

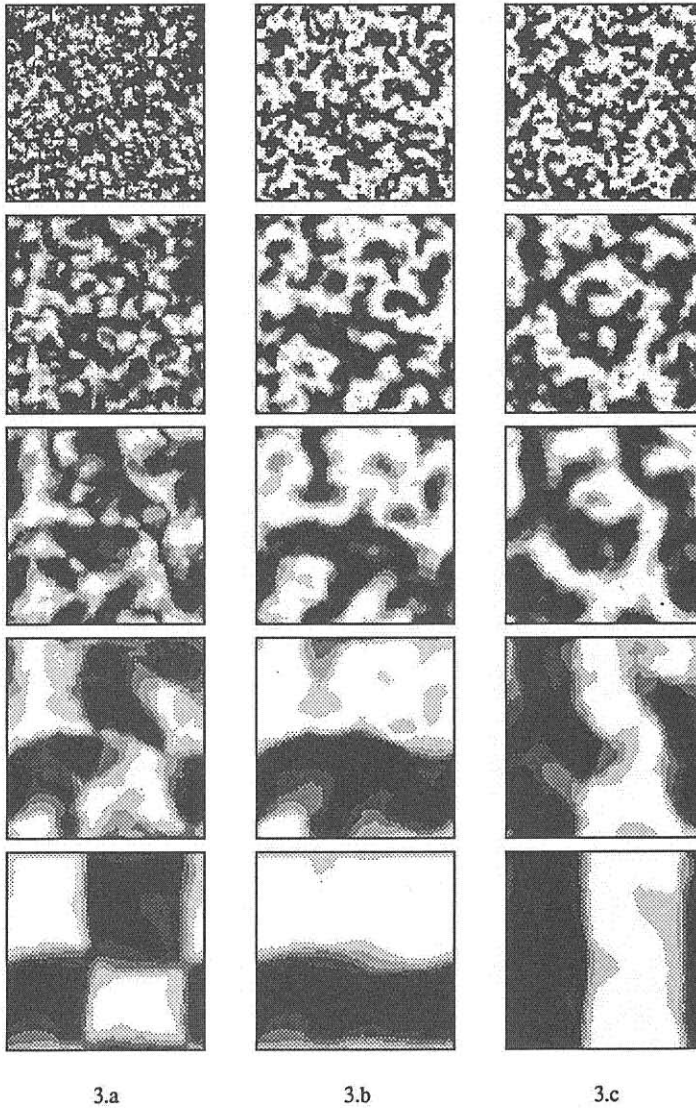


Figure 3: Time-averaged evolution of two initially random configurations for the ferromagnet at a temperature of 1.5. Times are from top to bottom 10, 50, 250, 1250, and 6250. (a) Time-averaged distance  $c_i(t)$  between the two configurations. (b) Time-averaged magnetization of the first configuration  $m_i(t)$ . (c) Time-averaged magnetization of the second configuration  $m'_i(t)$ .



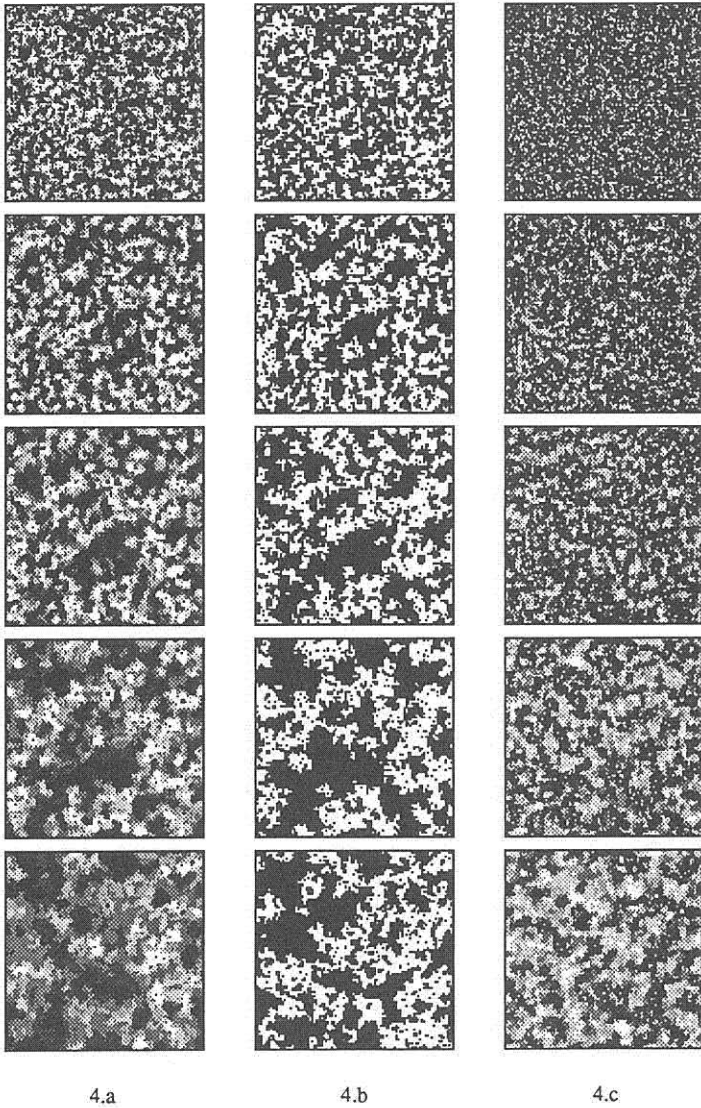


Figure 4: Time evolution of two initially random configurations for a symmetric spin glass at a temperature of 0.9. Times are from top to bottom 10, 50, 250, 1250, and 6250. (a) Time-averaged distance  $c_i(t)$  between the two configurations. (b) Instantaneous distance  $d_i(t)$  between the two configurations. (c) Flipping rate of the second configuration  $f_i(t)$ .

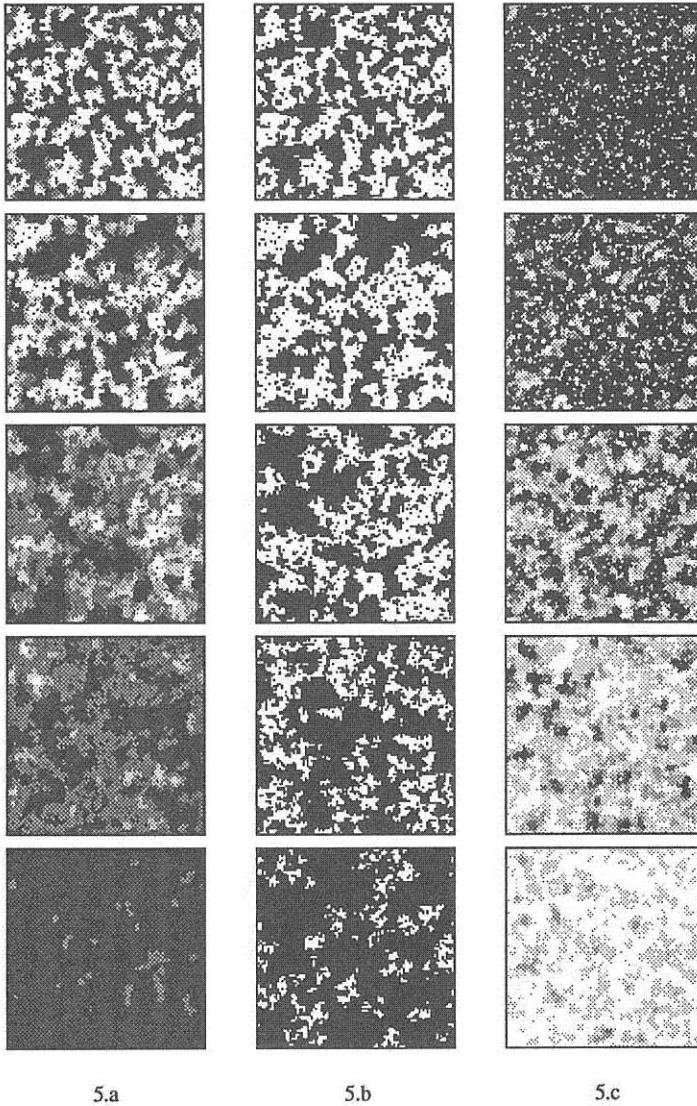


Figure 5: Evolution of two initially random configurations after 6250 time steps as a function of temperature for a symmetric spin glass. Temperatures are from top to bottom 0.3, 0.6, 0.9, 1.2, and 1.5. (a) Time-averaged distance  $c_i(t)$  between the two configurations. (b) Instantaneous distance  $d_i(t)$  between the two configurations. (c) Flipping rate of the second configuration  $f_i(t)$ .

$T_c \approx 1.56$  [3]. Far less structure is observed than in the symmetric case. The distance reaches equilibrium faster. The domain structure is smaller than for symmetric spin glasses. The nearly uniform grey level of the average distance show that these structures are extremely mobile. The bottom frame of the flipping rate is almost completely white, showing that no spin is frozen. The same behavior is observed at lower temperatures down to  $T = 0.01$ . As for the other cases, above  $T_c$ , the two configurations merge and all the spins are flipping.

## 6. Conclusions

In this work, we have seen that the three systems: ferromagnet, symmetric spin glass, and non-symmetric spin glass have rather different behaviors. The two extreme cases are clearly the ferromagnet and the non-symmetric spin glass. For the ferromagnet, we have seen that the structures associated with the distance are comparable in size and shape, to the magnetic domains. These domains do not move much in time. For the non-symmetric spin glass, the dynamics are much more chaotic. No spins are frozen, but there are small domains of opposite spins which move rather quickly. The symmetric spin glass has intermediate properties: rather large domains are associated to the distance. These domains are mobile but much less than in the non-symmetric spin glass. There are also some frozen spins at least at times  $t < 6250$ . The size of domains of frozen spins seems much smaller than the structures associated to the distance.

Another way of visualizing the growth of the domains associated to the distance for spin glasses is to start from a stripped structure represented on figure 7: we start with two configurations which are identical outside an horizontal strip, and opposite inside. We see that the strip of opposite spins invades the whole system. This invasion is much faster for the non-symmetric spin glass (column c) than for the symmetric spin glass (column a) when one starts with a random initial configuration. When starting from a configuration which has already evolved for 6250 time steps, the invasion for the symmetric spin glass is even slower and the structure appears more compact (column b). This invasion behavior has the same origin as the spreading of damages [17–19].

It would be interesting to try to observe domains on much larger samples in order to measure their fractal properties and to compare these observations for spin glasses with recent theories on domain structures [20–22].

It would also be interesting to redo similar calculations for other systems (Kawasaki dynamics, ANNNI model, boolean automata, etc.) to see whether they present new dynamical properties or they have a behavior similar to one of the models studied here. Lastly, since the structures associated to the distance are rather often mobile, it would be interesting to define a quantity which would give a measure of these motions. This might not be too easy because the clusters of opposite spins move, change in shape and disappear.

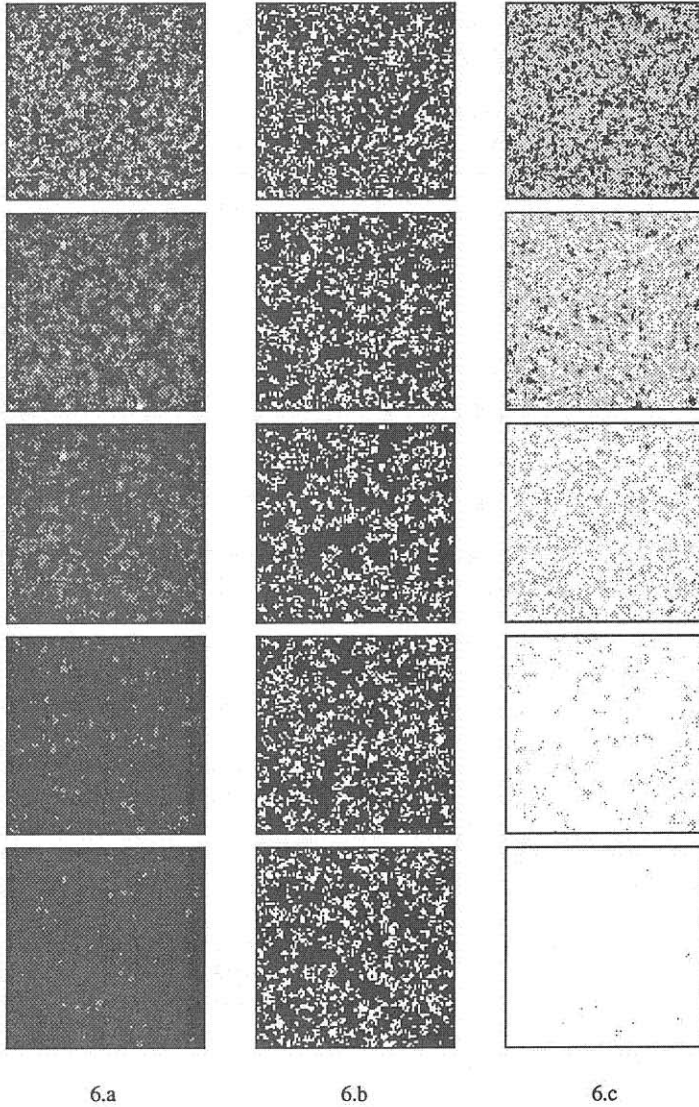


Figure 6: Time evolution of two initially random configurations for a non-symmetric spin glass at a temperature of 0.9. Times are from top to bottom 10, 50, 250, 1250, and 6250. a) Time averaged distance  $c_i(t)$  between the two configurations. b) Instantaneous distance  $d_i(t)$  between the two configurations. c) Flipping rate of the second configuration  $f_i(t)$ .

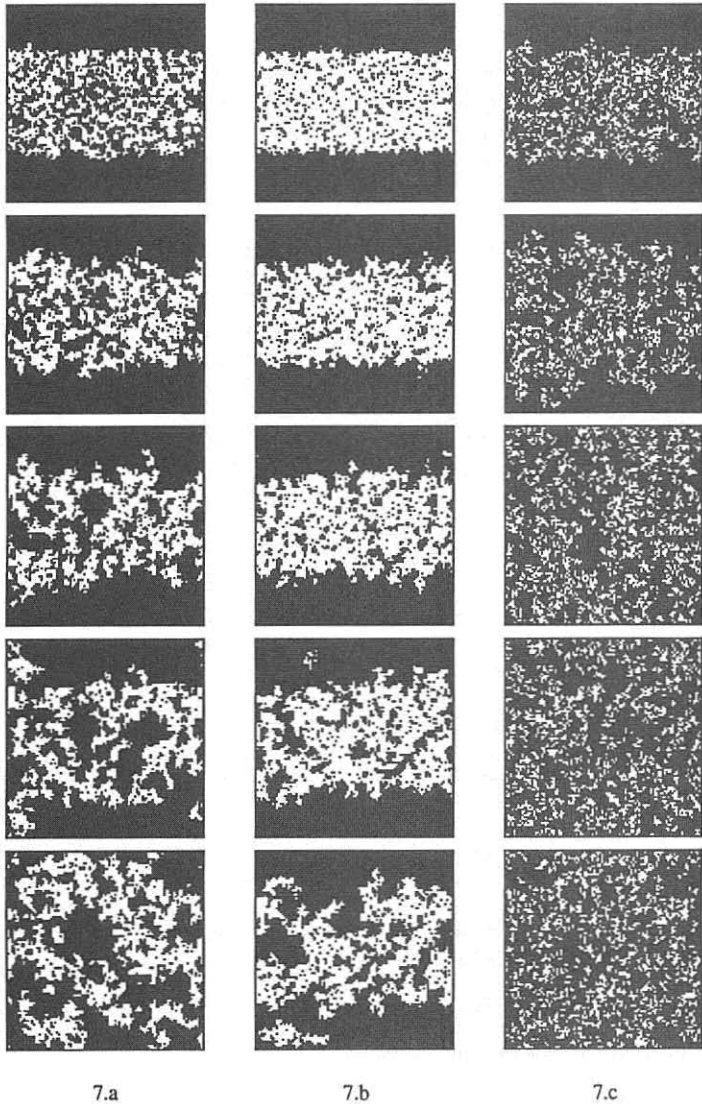


Figure 7: Time evolution of instantaneous configurations starting from two configurations which initially are half opposite on a horizontal strip. Times are from top to bottom 10, 50, 250, 1250, and 6250. a) Symmetric spin glass at a temperature of 0.9, with random initial configurations. b) Symmetric spin glass at a temperature of 0.9, with a 6250 steps old initial configurations. c) Non-symmetric spin glass at a temperature of 0.9, with random initial configurations. In all three cases, the difference spreads.

## Acknowledgments

We would like to thank Mrs. Claudine Verneyre for her help in graphics at an early stage of this work. This work was supported by BRAIN grant ECC (ST 2J - 0422 - C).

## References

- [1] B. Derrida and G. Weisbuch, "Dynamical Phase Transitions in 3-dimensional Spin Glasses," *Europhysics Let*, **4** (1987) 657.
- [2] O. Golinelli and B. Derrida, "Effect of thermal noise and initial conditions in the dynamics of a mean field ferromagnet," *Journal de Physique*, **49** (1988) to appear.
- [3] A. U. Neumann, B. Derrida, "Finite size scaling of dynamical phase transition in two dimensional models: ferromagnets, symmetric and non-symmetric spin glasses," *Journal de Physique*, **49** (1988) to appear.
- [4] M. N. Barber and B. Derrida, "Dynamical Phase Transitions in the two dimensional ANNNI model," *Journal of Statistical Physics*, **51** (1988) 877.
- [5] B. Derrida and G. Weisbuch, "Evolution of overlaps between configurations in random Boolean networks," *Journal de Physique*, **47** (1986) 1297.
- [6] G. Weisbuch and D. Stauffer, "Phase Transitions in cellular random Boolean nets," *Journal de Physique*, **48** (1987) 11.
- [7] B. Derrida and D. Stauffer, "Phase Transitions in two dimensional Kauffman cellular automata," *Europhysics Let*, **2** (1986) 739.
- [8] L. De Arcangelis, "Fractal dimensions in three-dimensional Kauffman cellular automata," *Journal of Physics*, **A20** (1987) L369.
- [9] D. Stauffer, "Random Boolean networks: analogy with percolation," *Philosophical Magazine*, **B56** (1987) 901.
- [10] A. Coniglio and L. De Arcangelis, "Hamiltonian formulation and critical temperature in Kauffman cellular automata," preprint 1988.
- [11] B. Derrida, E. Gardner, A. Zippelius, "An exactly solvable asymmetric neural network model," *Europhysics Let*, **4** (1987) 167.
- [12] B. Derrida and R. Meir, "Chaotic behavior of a layered neural network," *Phys. Rev. A* (1988) to appear.
- [13] K. E. Kürten, "Critical phenomena in model neural networks," *Physics Letter A*, **129** (1988) 157; "Correspondence between neural threshold networks and Kauffman Boolean cellular automata," *J. Phys.*, **A21** (1988) L615.
- [14] B. Derrida, "Dynamical Phase Transitions in non-symmetric Spin Glasses," *J. Phys. A20* (1987) L 271.

- [15] J. D. Gunton, M. San-Miguel, and P. S. Sahni, "The dynamics of first-order phase transitions" in *Phase Transitions and Critical Phenomena* eds. C. Domb and J.L. Lebowitz, vol. 8 (Academic Press, 1983).
- [16] J. L. Lebowitz, private communication
- [17] H. E. Stanley, D. Stauffer, J. Kertész, and H. J. Herrmann, "Dynamics of spreading phenomena in two-dimensional Ising models," *Phys. Rev. Let.*, **59** (1987) 2326.
- [18] U. M. S. Costa, "Spreading of 'damage' in a three-dimensional Ising model," *J. Phys. A20*, (1987) L583.
- [19] L. R. da Silva and H. J. Herrmann, "Damage spreading in a gradient," preprint 1988.
- [20] A. J. Bray and M. A. Moore, "Scaling theory of the ordered phase of spin glasses," *Heidelberg Colloquium on Glassy Dynamics, Proceedings*, (Springer Verlag, Heidelberg, 1986) 121.
- [21] G. J. M. Koper and H. J. Hilhorst, "A domain theory for linear and nonlinear aging effects in spin glasses," *Journal de Physique*, **49** (1988) 429.
- [22] D. S. Fisher and D. A. Huse, "Ordered phase of short-range Ising spin-glasses," *Phys. Rev. Let.*, **56** (1986) 1601.